Flow, Turbulence and Combustion (2021) 107:781–809
https://doi.org/10.1007/s10494-021-00252-3

Unsteady Effects on NO_x Measurements in Pulse Detonation Combustion

Niclas Hanraths[1] · Myles D. Bohon[2] · Christian Oliver Paschereit[3] · Neda Djordjevic[1]

Received: 4 August 2020 / Accepted: 9 February 2021 / Published online: 4 March 2021

Abstract
Emission measurements from unsteady combustion systems such as Pulse Detonation Combustion (PDC) are challenging due to the inherently large variations in pressure, temperature, composition, and flow velocity of the exhaust gas. Comparison of experimental data is additionally complicated by differences in operating conditions and gas sampling setup between different facilities. Qualitative considerations with regard to the sampling process from PDC, based on one-dimensional simulations, indicate a systematic influence of the sampling setup and extraction process on the resulting concentration measurements. Therefore, operating frequency, sample time, fill time, as well as PDC outlet and probe geometry were varied experimentally in order to assess the degree to which each of these parameters impact the resulting measured NO_x in order to better inform researchers of these effects when making measurements. It was shown that measured NO_x emissions can vary significantly depending on the choice of these parameters and therefore care must be exercised in order to reduce the influence of the sampling technique when aiming for comparable results.

Keywords Pulse detonation combustion · NO_x · Emission measurement · Transient gas sampling

1 Introduction

Combustion systems are required to become increasingly more efficient, while at the same time allowing for compact and easily maintained designs suitable for a more decentralized energy infrastructure. Because pressure gain combustion (PGC) systems can potentially

✉ Niclas Hanraths
niclas.hanraths@tu-berlin.de

[1] Technische Universität Berlin, Chair of Combustion Kinetics, Müller-Breslau-Str. 8, 10623 Berlin, Germany

[2] Technische Universität Berlin, Chair of Pressure Gain Combustion, Müller-Breslau-Str. 8, 10623 Berlin, Germany

[3] Technische Universität Berlin, Chair of Fluid Dynamics, Müller-Breslau-Str. 8, 10623 Berlin, Germany

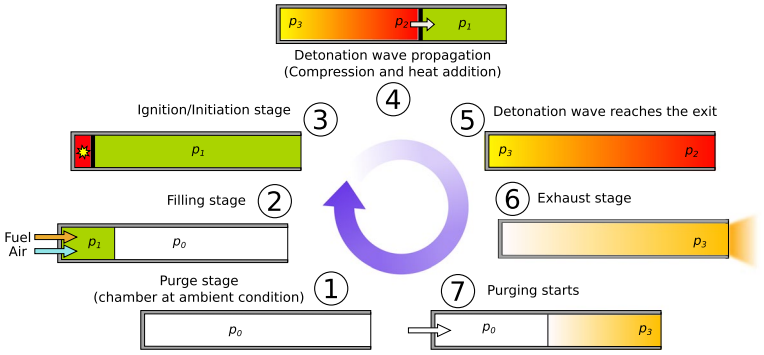

Fig. 1 Schematic depiction of a pulse detonation cycle

provide significant advances in all of these aspects, research interest towards fundamental research and practical applications remains strong.

One of the earliest concepts in PGC, pulse detonation combustion (PDC) was first introduced by Zel'dovich (2006) and is still investigated today as an alternative combustion method for aeronautic (Kailasanath 2000, 2003) and power generation purposes (Kailasanath 2009; Roy et al. 2004; Giuliani et al. 2010). Its main feature is the consumption of a premixed fuel-oxidizer mixture by a supersonic detonation wave traveling through the combustion chamber. This requires a cyclic operation with periods of purging and refilling, as depicted in Fig. 1. The combustion chamber primarily consists of a tube that is filled with a combustible mixture of fuel and oxidizer (2). Conventional combustion by means of a spark plug is initiated (3). This is followed by a rapid deflagration to detonation transition (DDT), which is usually enhanced by constricting the tube's inner diameter or supporting shock focusing by geometry alterations. The developed detonation wave propagates (typically at a velocity of several thousand meters per second) (4), until it reaches the tube exit (5). Here, the leading shock wave is reflected as a rarefaction wave that initiates the blowdown or exhaust stage of the cycle. During this phase, the combusted gases are expanded and further accelerated towards the tube exit (6). As soon as the inner pressure has fallen back to the initial pressure (or even below due to an overexpansion of the combusted gases and a subsequent back flow), the cycle can be re-initiated (7). The range of pressure differences between each phase is significant. For stoichiometric H_2–air detonations starting from atmospheric conditions as encountered in this work, peak pressure of the shock wave is about 28 bar but quickly decreases to an equilibrium pressure after combustion (p_2) of roughly 16 bar. The final pressure of the combustion products (p_3) before the arrival of the first expansion wave from the tube exit depends on the upstream boundary conditions but typically ranges in between 5 bar and 10 bar.

More recent work was focused on the interaction of the PDC's outlet conditions with an attached turbine (Rouser et al. 2014), as well as the potential of detonation based rocket engines (Wang et al. 2015) and turbofan engines (Xisto et al. 2018). Other studies have targeted increased operating frequency and thermal power output (Frolov 2014), characterization of the acoustic signature of the PDC (Anand et al. 2018), and the facilitation of the detonation initiation process by means of shock waves (Driscoll et al. 2016).

However, in addition to its potentially significant increase in thermal efficiency through constrained heat release (Heiser and Pratt 2002), the harsh conditions behind

the detonation wave in terms of pressure and temperature also give rise to concerns with regard to pollutant formation, especially NO_x. Earlier numerical studies by the authors Djordjevic et al. (2017), Hanraths et al. (2018) indicate the potential for very high NO_x emissions from PDC, which could introduce serious concerns for practical applications of this technology but could be mitigated by appropriate dilution methods. These findings were confirmed by Xisto et al. when simulating a PDC based turbofan engine (Xisto et al. 2018). Yungster et al. (2004, 2006), and Yungster and Breisacher (2005) investigated NO_x emissions from PDC operated with hydrogen or Jet-A fuel for varying equivalence ratios and fuel charge lengths. Numerical simulations found high NO_x emissions for near-stoichiometric conditions which also showed a strong dependence on residence time. Altering the equivalence ratio to leaner or richer conditions significantly reduced NO_x values. Residence time dependence was also found to decrease for off-stoichiometric mixtures. Experimental validation was sought for equivalence ratios of $\phi = 0.8$ and $\phi = 1$ for PDC operating frequencies of $f = 28\,\text{Hz}$ and $f = 37\,\text{Hz}$. Although overall trends agree reasonably well, a direct comparison is made difficult by the cycle-averaged nature of the experimental results. Schauer et al. (2009) measured NO and CO emissions downstream of a PDC operated with an H_2 –air or ethylene-air mixture at $f = 10\,\text{Hz}$ and found them to be comparable to the numerical results from Yungster et al. (2004) and Yungster et al. (2006) in both scale and depicted trends. Frolov et al. (2011) also measured NO_x concentrations inside a methane-air fueled PDC with results below those of conventional combustion systems, which he attributed to the reduced combustion time and the rapid expansion during the exhaust stage in the PDC cycle.

Overall, direct comparison of experimental and numerical data on NO_x emissions from PDC in the literature is complicated by large differences in operating frequency, charge length, purge ratio and purge gas composition, and sampling positioning.

An additional challenge is posed by the fact that common technologies, regulations, and "best practices" for the extraction of exhaust gases for emission measurements have been developed primarily in the context of steady combustion systems and thus are difficult to apply to transient systems (Rasheed et al. 2011). This does not only apply to PDC but also to all other forms of unsteady combustion systems such as the pulse jet engine (Paxson and Kaemming 2014; Lisanti and Roberts 2016) or the shockless explosion combustion (Yücel et al. 2020), where recent approaches in emission measurements revealed a large scatter (Qatomah et al. 2018). A recent review study of pollutant emissions in various pressure gain combustors also comes to the conclusion that—due to the inherently unsteady nature of these devices—measurement biases are prevalent and a better understanding of these influences is necessary (Anand and Gutmark 2019).

The goal of this study is therefore a systematic investigation into the technical challenges and implications of gas sampling for emission measurements from the unsteady, cyclic combustion system in the PDC. The impact of several key parameters on developing a systematic sampling technique will be investigated. Considering the significant variation in experimental apparatus, operating cycle design, emissions analyzers, and sampling access, a single "best practice" recommendation is unfeasible. However, this work will endeavor to demonstrate the impact of these common sampling characteristics and thereby better equip researchers to reduce these systematic uncertainty and increase the comparability of their measurements.

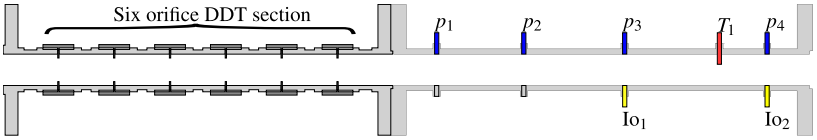

(a) DDT and measurement section, the latter equipped with PCB pressure transducers, ionisation probes and thermocouples

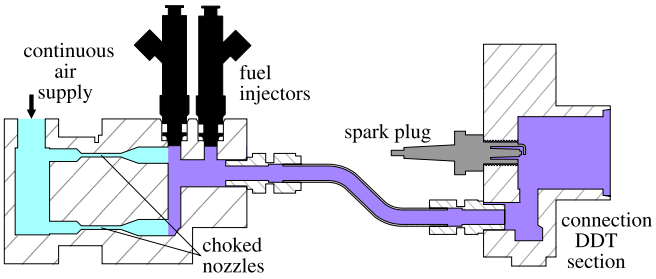

(b) PDC injection section

Fig. 2 PDC test rig

2 Experimental Setup

This section provides information about the experimental facilities of this study and allows for an overview of the operation conditions and investigated parameters.

2.1 PDC Test Rig and Gas Analyzer Capabilities

The current design of the PDC test rig is derived from the one that was developed and tested previously in Gray (2017), with the latest changes in design described in Völzke et al. (2019). The combustion chamber has an inner tube diameter of 30 mm and consists of an injection section (shown in detail in Fig. 2b), a deflagration to detonation transition (DDT) section, and a measurement section (Fig. 2a). Within the injection section, a fixed air mass flow of 36.1 g/s is mixed stoichiometrically with hydrogen supplied by three automotive injector solenoid valves. Mixing is enhanced by a jet in cross flow configuration of the fuel lines. Fill time was 35 ms unless otherwise noted, which guarantees that the combined length of the DDT section (630 mm) and measurement section (820 mm) is completely filled with combustible mixture. A spark plug is used to ignite the combustible mixture. Reliable DDT is achieved by the insertion of six orifice plates between the point of ignition and the beginning of the measurement section. Each orifice has a blockage ratio of 0.43 while the distance between orifices was 85 mm. Several ports along the measurement section are equipped with piezoelectric pressure transducers and ionization probes to measure the propagation velocity of the detonation front by time-of-flight. After the exhaust of the combustion products sufficiently reduces the pressure inside the tube, the air flow re-establishes and acts as purge gas.

To allow for emissions measurements, the exhaust of the test rig is equipped with a support tube holding the sampling probe. Three different probe designs were used. The layout of the baseline water-cooled sampling probe is depicted in Fig. 3. It has a cylindrical shape

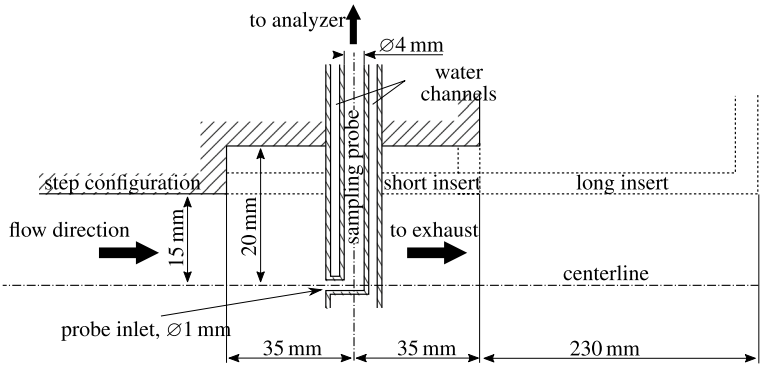

Fig. 3 Cross-sectional view of sampling system (not to scale) with illustrations of the variation in the combustor tube outlet geometry through the inclusion of various short or long inserts

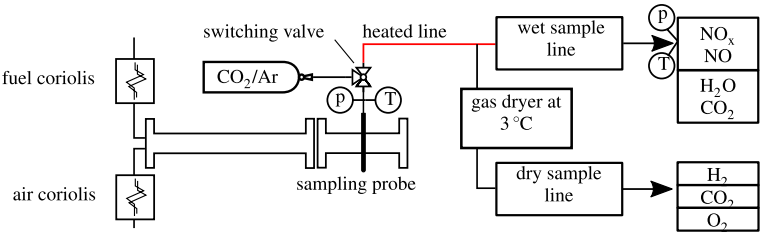

Fig. 4 Emission measurement analyzer setup

with an outer diameter of 10 mm and extends across the entire diameter of the tube. The inner sample tube containing the sample gas has an inner diameter of 4 mm and a 1 mm sampling orifice. The inlet can be traversed across the tube diameter. The sample orifice can be aligned either in the flow direction or at a variable angle to it. The second probe design consists of a thin, pitot shaped tube with a sharpened tip to allow for gas sampling with a minimum of flow disturbance. The third design is flush mounted in the combustion chamber wall, perpendicular to the flow. All probes have the same orifice size and are equipped with water circulation channels to maintain a constant wall temperature.

Figure 4 shows the gas analyzer setup that is connected to the sampling probe through a 0.5 m heated sample line at 190 °C. This allows for NO_xmeasurements on a wet basis within the subsequent chemiluminescence detector (KNESTEL CLD dual BASIC). The wet sample line is also equipped with a nondispersive infrared sensor (NDIR) capable of measuring CO_2 and water content to account for chemiluminescent quenching inside the CLD reaction chamber. Pressure and temperature of the gas are measured between the probe and the heated sample line by a piezoresistive pressure sensor and a Type-K thermocouple, respectively. Additional pressure and temperature sensors are located at the inlet of the CLD. The CLD was calibrated to measurement ranges of 0 to 500 ppm and 0 to 2500 ppm using calibration gases of 500 and 1000 NO in N_2, respectively.

In parallel to the wet sample line, a dried gas sample is used for measuring the oxygen, hydrogen, and CO_2 content by means of a paramagnetic sensor (ABB Magnos 106), a thermal conductivity sensor (ABB Caldos 27), and an NDIR sensor (ABB Uras 14),

respectively. Both the wet and dry sample lines are each equipped with a gas vacuum pump drawing in sample gas at a constant volumetric flow rate of 7.2 l/h and 60 l/h, respectively.

It is important to point out that, even for comparably low operating frequencies, none of the measurement equipment in the gas analysis section of the test rig is able to accurately capture the small time scales involved in one cycle of a PDC. The CLD displays a response time of less than a second. In combination with the time delay introduced by the length of the sample line and the measurement train, which is of the same magnitude, the maximum recognizable frequency of the emission system is of the order of 1 Hz. Hence, all information acquired through these analyzers is averaged over the course of many cycles.

All analyzers require a constant supply of sample gas. As a consequence, if sampling times are to be varied during PDC operation, a solenoid switching valve is placed downstream of the sampling probe to select the source of the sampled gas from either the combustion chamber or a diluent in the form of a mixture of 25% CO_2 in Ar.

2.2 Remarks on Gas Concentration Measurements in an Unsteady Flow Field

This section addresses the systemic challenges that are posed by emission measurements in a pulsed combustion environment. Eventually, the purpose of all emission measurements is to quantify the amount of pollutant particles (or pollutant mass) that a specific combustion process releases into the environment. In most cases, an analysis of the total amount of exhaust gases is neither feasible nor necessary. Instead, continuous emissions monitor (CEM) systems usually extract small gas samples under controlled conditions, with the actual measurement producing the pollutant concentration within this sample volume. To still allow for conclusions with regards to the total amount of emitted pollutants, it must be ensured that the composition of the sample is representative of the composition of the total flow. For systems that show a steady-state behavior, both in terms of combustion and their flow field, this usually does not pose a problem, provided that exhaust gases are sufficiently spatially homogeneous at the sampling position and that sample composition is not influenced by the flow field in the vicinity of the sampling probe.

However, experimental assessment of pollutant emissions from PDC requires extracting gas samples from a highly transient flow with cyclic combustion events. This creates several challenges for the traditional concept of emission sampling: The first issue arises from the fact that all flow properties are now varying with time during each combustion cycle. The lack of a steady-state value leaves two choices to adequately quantify the emission of measured pollutants from the system: Either measurements must be able to provide time-resolved species concentration data, or a sensible reference value that incorporates all temporal variations must be defined. The former is usually not feasible since most CEM systems exhibit a considerable delay in the range of several seconds due to their measurement principle, large internal volumes in the sample train, or the method of gas sampling. Thus, when using these systems in the context of cyclic combustion such as PDC, the resulting concentration measurements will only represent a quasi-steady-state average result. This leads to the second issue, which is whether the obtained average concentration is a faithful representation of the total pollutant emission per cycle and thus the desired sensible reference value. As will be shown, this primarily depends on how well the supply of sample gas to the sampling system is able to capture the temporal variations of the exhaust gases.

A faithful representation of the amount of NO_x from a combustion system would allow one to deduce the total amount of emitted pollutants n_{NO_x} in relation to the overall mole

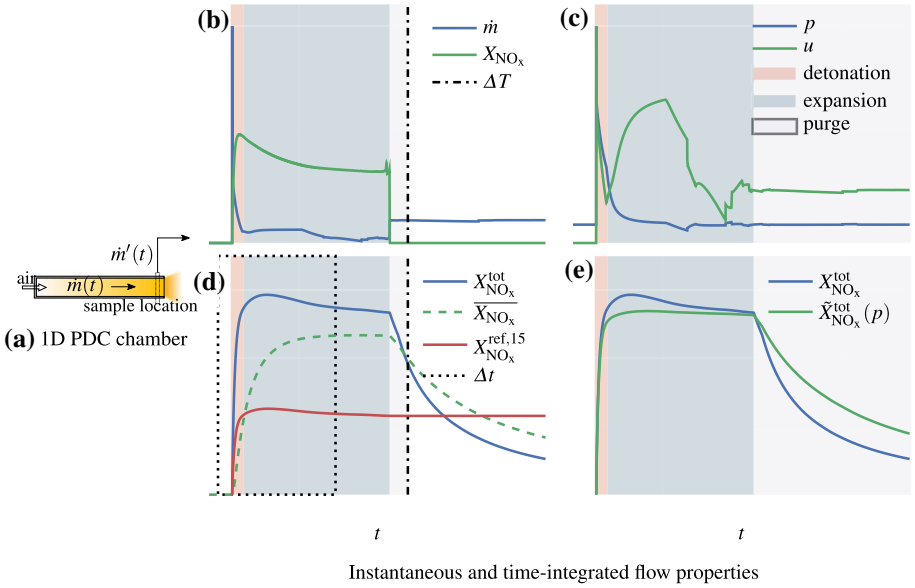

Fig. 5 Influence of unsteadiness on gas sampling from PDC exhaust stream

output of the system n during a defined amount of time, thus it should be possible to derive the total mole fraction

$$X^{\mathrm{tot}}_{\mathrm{NO_x}} = \frac{n_{\mathrm{NO_x}}}{n}.$$

For transient systems, the total amount of moles must be regarded as the time integral of the corresponding fluctuating molar flow rates so that

$$X^{\mathrm{tot}}_{\mathrm{NO_x}}(t) = \frac{\int_{t_0}^{t} \dot{n}_{\mathrm{NO_x}}(\tau)\,d\tau}{\int_{t_0}^{t} \dot{n}(\tau)\,d\tau} = \frac{\int_{t_0}^{t} X_{\mathrm{NO_x}}(\tau)\,\dot{n}(\tau)\,d\tau}{\int_{t_0}^{t} \dot{n}(\tau)\,d\tau}. \tag{1}$$

However, with both the total mole fraction $X_{\mathrm{NO_x}}$ and $\dot{n}$ being functions of time, the resulting $X^{\mathrm{tot}}_{\mathrm{NO_x}}$ depends on the chosen integration period.

To illustrate this, Fig. 5 uses results from a one-dimensional simulation of a detonation wave, as already employed for similar conditions in Hanraths et al. (2018). Here, the detonation itself is regarded as a planar, one-dimensional phenomenon in accordance with the ZND model[1] that can be represented within the frame of the reactive Euler equations, that is, as an inviscid and nonconductive but chemically reacting compressible fluid. To this end, the simulations apply an HLLE approximate Riemann solver in parallel to the multi-step chemistry of the H_2–O_2 kinetic mechanism by Burke et al. (2012), which has been extended by the San Diego NO_x submechanism (Hewson and Bollig 1996). The numerical domain represents a simplified combustion chamber with a continuous air supply as

[1] Named after its three independent proposers (Zel'dovich 2006; Von Neumann 1942; Döring 1943).

depicted in Fig. 5a, where the gas sampling process is emulated by tracking the flow properties close to the chamber outlet. Before ignition, the chamber is completely filled with a combustible H_2–air mixture. A precalculated ZND profile is used to initiate the detonation at the left boundary of the domain. After propagating through the tube and exiting towards the environment (detonation phase), the open end boundary condition causes an expansion wave that reduces the post-combustion pressure until it falls below the supply pressure of the continuous air supply (expansion phase). The ensuing purge phase replaces the remaining combustion products inside the combustion chamber with air (purge phase).

The graphs of Fig. 5b–e depict the temporal evolution of flow properties such as mass flow $\dot{m}$, NO_x mole fraction X_{NO_x}, pressure p, and gas velocity u at the sampling position during a full PDC cycle. Since the following discussion is aimed at a qualitative analysis of their time dependent behavior, scales are omitted. The initial detonation induces a strong peak in the mass flow $\dot{m}$ that is followed by expansion waves that cause the flow to exit from the combustion chamber. Eventually, a constant air mass flow reestablishes during the purge phase. The distinct phases are indicated by colored areas. Even though the detonation phase displays the steepest gradients, due to its short duration most of the NO_x molecules are encountered during the expansion phase until the point that the concentration drops sharply when purging ensues.

Due to the high temperatures and the sufficient availability of O_2 for near-stoichiometric detonations, NO formation is dominated by the thermal path. In this case, a coarse estimate of the kinetic time scale of NO formation is given in Heywood (1988) by

$$\tau_{NO} = \frac{8 \times 10^{-16} T \exp\left(\frac{58300}{T}\right)}{\sqrt{p/101325}}. \tag{2}$$

While peak values of temperature and pressure within a stoichiometric H_2–air detonation wave can reduce this to $\tau_{NO} \approx 7$ ms, these conditions only last for far less than 1 ms. Therefore, combustion product conditions after the main heat release has already occurred and during the subsequent expansions waves are the defining ones to estimate τ_{NO}, which results in values of the order of $\tau_{NO} \approx 150$ ms. Comparing this to the typical particle velocities of the combustion products that range between 100 and 1000 m/s, resulting in residence times on the order of 30 ms, it becomes clear that, even though thermal NO forms relatively fast during the short and intense detonation phase, residence time within the combustion chamber is insufficient to reach equilibrium conditions except for very long tubes.

With the combustion chamber assumed to be fully filled with combustible mixture and its length fixed, the chosen cycle duration ΔT (that is, the period of the PDC operating frequency f) defines the length of the purging phase.

As a result, the integral value of $X^{tot}_{NO_x}$ is primarily influenced by the length of the purge phase and continuously declines for increasing cycle length ΔT. It is worth pointing out that due to the strong variations in mass flow, the value of $X^{tot}_{NO_x}$ calculated using Eq. 1 is distinctively different from a simple time averaged mole fraction defined by

$$\overline{X_{NO_x}}(t) = \frac{\int_{t_0}^{t} X_{NO_x}(\tau)\, d\tau}{\int_{t_0}^{t} d\tau}. \tag{3}$$

As can also be seen in Fig. 5d, correcting the absolute pollutant concentrations to a fixed exhaust oxygen content of 15 vol% allows for elimination of the effect of increased air

dilution during longer purge phases, as the corrected value remains constant. This effectively results in a total concentration value $X_{\mathrm{NO_x}}^{\mathrm{ref,15}}$ that is independent of operating frequency as long as the sampling window captures all combustion products and lasts into the purge phase. Similarly, limiting the sampling of exhaust gas to a certain sampling time window defined by Δt can have a strong influence on the measured reference concentration, because phases of high pollutant concentration are omitted in the investigated gas sample.

Additionally, all of the above considerations and equations account for the entirety of the bulk flow of the exhaust gases, even though a practical gas sample would extract only a small sample mass flow $\dot{m}' \ll \dot{m}$, as illustrated in Fig. 5a. Consequently, Eq. (1) would change to

$$X_{\mathrm{NO_x}}^{\mathrm{tot}}(t) = \frac{\int_{t_0}^{t} \dot{n}'_{\mathrm{NO_x}}(\tau)\, d\tau}{\int_{t_0}^{t} \dot{n}'(\tau)\, d\tau} = \frac{\int_{t_0}^{t} X_{\mathrm{NO_x}}(\tau)\, \dot{n}'(\tau)\, d\tau}{\int_{t_0}^{t} \dot{n}'(\tau)\, d\tau}, \tag{4}$$

when assuming that the sampling process itself has no direct chemical impact on the composition of the gas sample (e. g. by wall reactions or pressure drops within the sample line), species composition of both flows remains identical (i. e. $X'_i(t) = X_i(t)$ for all t). Equation (4) becomes equivalent to Eq. (1) only when

$$\frac{\dot{n}'}{\dot{n}} = \frac{\dot{m}'}{\dot{m}} = \text{const.}$$

However, in a practical implementation, it is reasonable to expect that $\dot{m}'$ is significantly influenced by the interaction of the flow field at the sampling position with the actual geometrical properties of the sampling probe and the specifics of the sampling train. An impression of the amount of variations in static pressure and velocity can be found in Fig. 5c. For the simplified assumption of a one-dimensional detonation with subsequent purging phase, the interaction of the contact surface with reflected shock and expansion waves creates a complex series of rapid changes in velocity. Even though purging in a real detonation chamber would most likely display a smoother development, rapid changes in the flow field are still to be expected and have been recorded in experiments as well. A simple model could assume the strength of the sample mass flow to be governed by the total pressure at the sample location, i. e.

$$\dot{m}'(t) \propto p_{\mathrm{tot}}(t).$$

Figure 5e includes the comparison of the temporal development of $X_{\mathrm{NO_x}}^{\mathrm{tot}}$ as defined by Eq. 1 and an assumed $\tilde{X}_{\mathrm{NO_x}}^{\mathrm{tot}}$ where $\dot{m}'$ scales linearly with pressure so that

$$\tilde{X}_{\mathrm{NO_x}}^{\mathrm{tot}} = \frac{\int_{t_0}^{t} X_{\mathrm{NO_x}}(\tau)\, p_{\mathrm{tot}}(\tau)\, \dot{n}(\tau)\, d\tau}{\int_{t_0}^{t} p_{\mathrm{tot}}(\tau)\, \dot{n}(\tau)\, d\tau}. \tag{5}$$

The resulting integral reference concentration diverges from the one based on the unaltered bulk mass flow in that the pressure decrease during the early expansion phase mitigates the maximum $\mathrm{NO_x}$ concentrations while the diminishing influence of dilution is less pronounced due to the lower pressures during the purge phase. This does not incorporate the effect of the considerable velocity variations that could cause additional sample flow fluctuations due to possible changes in stagnation pressure at the sample probe inlet.

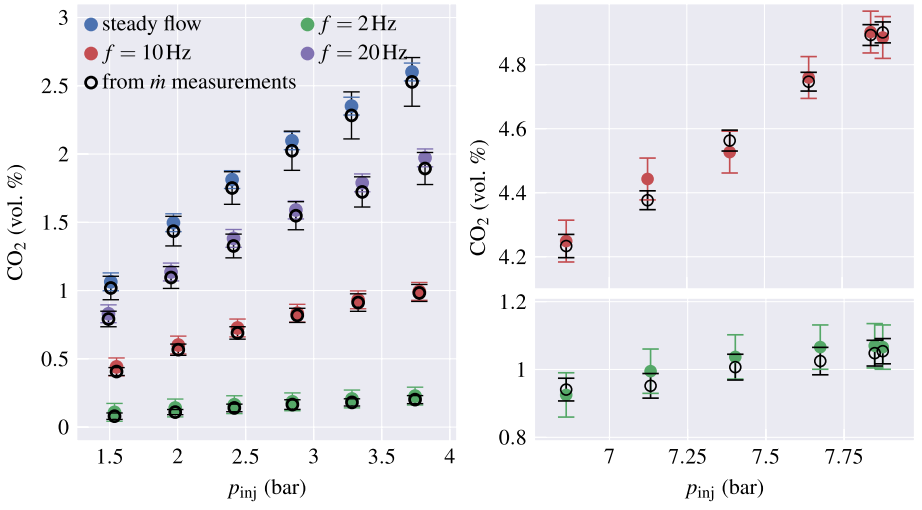

(a) inert: 25 %CO_2-75 %Ar in air **(b)** w/ combustion: 20 %CO_2-80 %H_2 in air

Fig. 6 Measured and expected CO_2 volume fractions with error bars signifying measurement uncertainty for gas analyzer measurements and cyclic fluctuations for mass flow measurements

Momentary changes of pressure at the sampling location could skew the resulting concentration measurements depending on the instantaneous bulk gas state.

As a consequence from these considerations, the integrity of the PDC gas sampling setup needed to be verified. For this purpose, measurements were carried out that involved the pulsed injection of inert gas into a PDC with a continuous air mass flow of 36.1 g/s. The inert gas used was a mixture of 25% CO_2 in Argon. Pulse frequencies of 2 Hz, 10 Hz and 20 Hz as well as steady injection were realized. During operation, the time-averaged mass flow of the inert gas as well as the air mass flow was recorded using a Coriolis mass flow meter upstream of the mixing section, as depicted in Fig. 4. These measurements allowed for the determination of the expected CO_2 concentrations in the exhaust gas, which could then be compared to the measured concentrations in the gas sample. Injection pressure p_{inj} was varied across a wide range to ensure that it had no influence on the comparability of injected to measured concentrations. The results are shown in Fig. 6a, with p_{inj} being directly proportional to the injection mass flow of the CO_2–Ar mixture. To allow for an assessment of the experimental uncertainties involved in this calibration, error bars of the mass flow measurement (black lines) denote mass flow fluctuations[2] during the measurement, whereas error bars for the concentration measurements (colored lines) derive from the measurement uncertainties as specified for each device.

Agreement is very good, with maximum deviations between mass flow and concentration measurements in the range of 3 to 5% of the measured value, independent of injection pressure and operating frequency. These deviations are fully covered by the uncertainties deriving from flow fluctuations and measurement uncertainty.

To also assess the impact of combustion reactions and shock waves on the sampling system, additional measurements with a mixture of 20% CO_2 in H_2 were conducted.

[2] Measurement uncertainties for Coriolis measurements turned out to be negligible in comparison

Table 1 Experimental parameters (defaults in **boldface**)

f	2 Hz	10 Hz	20 Hz	
$\dot{m}_{air}$	36.1 g/s			
fuel	H_2			
ϕ	1			
t_{run}	10 s	20 s	**30 s**	
t_{fill}	20 ms	**35 ms**	50 ms	75 ms
t_{ign}	t_{fill} + 5 ms			
α	**0°**	45°	90°	180°
Outlet geometry	Step	Short insert	**Long insert**	
Probe design	**Cylindric tube**	Pitot tube	Flush mounted tube	

Analogous to the inert experiments, the mixture was injected into a constant stream of air at varying frequencies. However, the mixture was ignited after filling of the combustion tube was complete. To allow for a combustible mixture, air mass flow rate had to be reduced to 22.2 g/s while injection pressure p_{inj} had to be increased. This made operating frequencies above 10 Hz unfeasible.

As before, measured CO_2 concentrations in the exhaust were compared to measurements of the inflow rates of air and CO_2–H_2obtained by the Coriolis mass flow meters. The depicted results in Fig. 6b show very good agreement within the the range of uncertainty for both 2 Hz and 10 Hz operating frequencies. Hence, confidence is lent to the fact that the sampling system itself, although only able to capture integral values, delivers representative data about the composition of the exhaust gas, even for pulsed combustion operation of increased frequency. However, it should be noted that due to the diluting influence of CO_2 the majority of the combustion events of which the results are shown in in Fig. 6b were fast deflagrations, not detonations. Nevertheless, those still led to the formation of shock waves of significant strength in any case.

2.3 Experimental Parameter Space

The goal of this study is to cover a wide range of possible factors influencing emission values measured from a PDC. This section briefly describes the parameter space of the study. Table 1 gives an overview of the constant and varied operating conditions, along with their default values.

PDC operating frequencies f of 2 Hz, 10 Hz, and 20 Hz were chosen for the experiments. However, some configurations did not allow for all frequencies to be investigated, especially in cases where higher frequencies resulted in emission levels outside of the measurement range of the analyzing equipment or when lower operating frequencies resulted in concentrations at the lower end of the resolvable concentration scale. Air mass flow $\dot{m}_{air}$, fuel and equivalence ratio ϕ were kept constant throughout this study, but their influence is the focus of on-going work.

The first preliminary experiments were targeted towards assessing the necessary experimental run time t_{run} to reach steady state conditions in terms of the chemical composition of the measured exhaust gas. Thus, the PDC run time was varied while also analyzing the influence of operating frequency. Critical measurement data to be investigated in that regard consisted primarily of the transient evolution of the measured species mole fractions

(NO_x, O_2, H_2) during the run duration. The measured detonation velocities were taken as confirmation that all shots within one measurement run were indeed successfully induced detonations. This is important as it has been observed that every disturbance in the mode of combustion (e. g. misfirings, unsuccessful DDT) is immediately reflected in the measurement of NO_x concentrations.

The default fuel injection period (t_{fill}) during each cycle was set to 35 ms, which is sufficient to fill the entire PDC tube with combustible mixture prior to ignition. To prevent flashback, a delay of 5 ms was employed before ignition to allow an air buffer between the filling section and the actual combustion zone. The impact of varying t_{fill} on measured gas species concentrations was investigated.

The choice of a specific sampling time window Δt during each PDC cycle could be necessary, especially for low operating frequencies that allow for more flexible sampling timings due to the extended duration of a single detonation cycle. If t_{fill} is held constant, lower frequencies experience increased dilution of the gas sample by the longer sampling of purge air in the exhaust. Due to the valveless nature of the combustion chamber air supply, the contact surface between combustion products and purge air within the detonation tube is subject only to the internal flow field and thus depends on the individual pressure development during and after each detonation. As a result, the noticeable onset of the purge phase might change between cycles, possibly altering the overall emission behavior. Therefore, it could be desirable to define a repeatable measurement window during the combustion cycle while still obtaining a sufficiently large amount of sample gas.

Other experiments investigated the influence of the proximity of the sampling location to the combustion chamber outlet. These different geometries are referred to as the *step design*, the *short insert*, and the *long insert* and can be seen in Fig. 3. The step design involves a sudden step-like increase of the detonation chamber's diameter from 30 to 40 mm, 35 mm upstream of the sampling probe's inlet. The second one uses a short insert to maintain a constant inner diameter of 30 mm until the tube opens towards the environment (35 mm downstream of the sampling probe). The third one extends the tube by 230 mm, thus increasing the distance between sampling point and tube exit. The distance between the point of fuel injection, the ignition location, and the sampling location all remain the same for all three geometries.

The cylindrical sampling probe also allowed for a variation in the alignment of the main flow within the combustion chamber and the orifice of the gas sampling probe, so that the bulk flow velocity of the gases would approach the probe in a different angle α.

Finally, the geometry of the probe itself was changed to less intrusive designs such as a pitot tip and a flush mounted design, allowing for an estimation of the impact of a blunt body shape on the high velocity flow downstream of the detonation front with respect to emission measurements.

3 Results and Discussion

Experimental measurements were conducted to investigate the significance of the parameters discussed in the previous section with regard to emissions measurements. Measurements for each configuration were repeated three times, the mean value of which is shown as a solid line or markers while the resulting standard deviation between repetitions is indicated by error bands or error bars. To ensure a wider comparability of the measured NO_x concentrations and account for different amounts of air dilution of the combustion exhaust

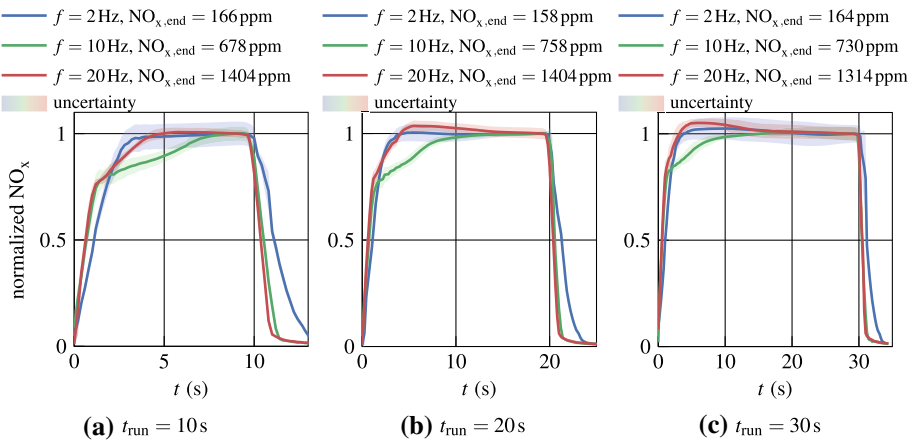

Fig. 7 NO_x concentrations normalized by their approached steady state value over time $NOx_{,end}$ for varying PDC run times

gases as discussed in the previous section, these concentrations are additionally displayed when corrected to a fixed exhaust oxygen concentration. For stationary gas turbines and similar systems, this is commonly chosen to be 15 vol% on a dry basis (European Council 2010; U.S. Environment Protection Agency 1993). Additionally, excess H_2 in the exhaust gas was mathematically removed as well. However, due to the H_2 analyzer being limited to a span of 2%vol, the latter becomes less reliable for large quantities of H_2. The full formula for correcting the measured concentrations to reference conditions thus becomes

$$X_{\text{corrected}} = \frac{20.94 - \mathrm{O}_{2,\text{ref}}\%}{20.94 - \mathrm{O}_2\%} \frac{100}{100 - \mathrm{H_2O}\%} \frac{100}{100 - \mathrm{H}_2\%} X_{\text{uncorrected}} \tag{6}$$

Note that results reach a singularity when oxygen content in the exhaust approaches atmospheric conditions (that is, for high dilution rates or low operating frequencies). Thus, it becomes very sensitive to small fluctuations in measured O_2 concentrations for these cases, which results in measurement uncertainties that become very large. Corrected concentrations are indicated as $NO^{15\%}$ and $NO_x^{15\%}$.

3.1 Reaching Steady State Conditions

Due to the differences in operational time scales discussed in the previous section, the interaction of a fluctuating PDC exhaust gas flow with a subsequent CEM is to a certain extent unknown. Therefore, the first task in the course of this study was to investigate the response time of the sampling system and identify the settling time of the combined sampling train and the analyzers for several PDC operating frequencies to ensure that each experimental configuration was able to provide unambiguous results in terms of emission measurement. Figure 7 shows the temporal development of the measured NO_x concentrations, normalized by the measured value averaged between 60% and 93% of each run time for varying operating frequencies and PDC run times.

Notable differences in the rise behavior of the signal can be found that result from the strong dependence of measured NO_x concentrations on the operating frequency: While

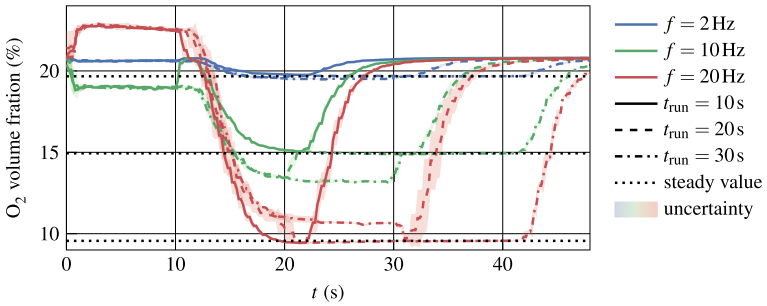

Fig. 8 Time development of measured O_2 volume fraction for varying PDC run time

10 Hz and 20 Hz result in rise rates in excess of the sensor response time, leading to identical initial surges followed by a more moderate adjustment period to the final steady-state value, the overall signal for 2 Hz is a lot smoother. Another result of this behavior is the fact that measured NO_x values tend to initially overshoot for the cases of 20 Hz and undershoot for 10 Hz. Nevertheless, all examined frequencies provide sufficiently stable NO_x concentrations for run times of 20 s and 30 s, in the sense that relative temporal standard deviation during the averaged steady-state time window was reduced to below 1%, which is of the same scale as the accuracy of the CLD analyzer. The relative spread of the results is mostly constant across the investigated frequencies, with a slight increase for the 2 Hz case due to the reduced signal strength for lower concentrations.

Sufficiently steady signals must also be ensured for the measurement of O_2 through the paramagnetic sensor in order to correct for the exhaust O_2 concentration.

Figure 8 shows the measured O_2 volume fractions over time, again for varying PDC run times and operating frequencies. The most important information to be derived from Fig. 8 is the fact that all curves obtained for the same operating frequency coalesce towards a common, stable oxygen volume fraction, independent of run time (indicated by dotted black lines). However, reaching this value requires considerably more time compared to the NO_x signal due to the fact that the paramagnetic sensor is located farther downstream of the sample line (larger volume) and also has a longer response time. For this reason, the sensor does not report any change in composition until approximately 10 s of PDC run time have already elapsed, independent of frequency or total run time length.

Due to less sampled purge gas over the course of a cycle at different operating frequencies, a clear frequency dependence is also visible, with the oxygen content of the exhaust gas reaching a minimum for the highest operating frequency.

Also, a sudden jump in the measured oxygen content is apparent at the start of the PDC operation ($t = 0\,\mathrm{s}$) and at the end of each run (at $t = 10\,\mathrm{s}$, $t = 20\,\mathrm{s}$, and $t = 30\,\mathrm{s}$). These jumps are the result of strong vibrations induced to the casing of the gas analyzer by pressure waves leaving the combustor during the operating time of the PDC and thus mark their onset and conclusion during the course of a run. Because the paramagnetic O_2 sensor is of the magnetomechanical type, its inner test body is susceptible to vibrations that can cause oscillations and thus indicate a change in oxygen content. Depending on the frequency, this error can indicate an increase or decrease in O_2, as can also be found in Fig. 8. Nonetheless, since measured oxygen concentrations between varying operating time (i. e. exposure time to vibrations) agreed remarkably well and no noticeable drift in the baseline value could be found, it can be concluded that this shift is only temporary in nature and has no lasting effect on the measurement result, as long as care is taken in the choice of

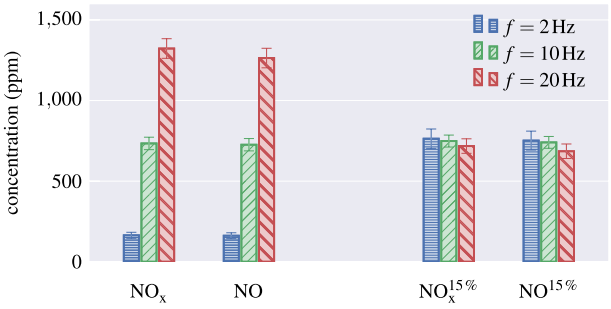

Fig. 9 Sample average of measured NO_x concentrations for varying PDC operating frequency

a time frame that omits this behavior. Thus, only the resultant stable oxygen values after PDC operation has ceased were considered to determine the oxygen content of each sample (indicated by the horizontal dotted lines in Fig. 8).

Similar to the requirements with regard to a minimized fluctuation of the measured NO_x and NO signals discussed before, a PDC operating time of 20 s is typically sufficient to obtain a stable period of measured O_2 concentration, after the aforementioned vibrations have stopped. Nevertheless, to ensure that the initial transient behavior found in both measured species concentrations does not affect time-averaged reference values, a PDC operating time of 30 s was chosen as the reference values for all the following experiments. A steady-state reference value for each configuration was derived by taking a time-average of the measured signal between 18 s and 28 s after the initial rise in NO_x (21 s and 31 s for O_2 due to the additional delay). It is worth pointing out that these numbers are specific to the experimental setup and should be adjusted if changes in the laboratory configuration—such as the distance between devices—are made. Researchers are therefore encouraged to independently confirm their own system specific response and settling time.

3.2 Influence of Operating Frequency

Figure 9 shows the measured concentrations of NO_x in absolute terms, as well as corrected to an oxygen content of 15% on a dry basis. As for the oxygen content, measured NO_x emissions strongly depend on the chosen operating frequency for uncorrected concentrations. Since all frequencies were operated using the same fuel injection timing, and thus primarily differ in the amount of purge air between ignitions, this is to be expected. Figure 9 confirms that this dependence is indeed linear for absolute NO_x measurements.

When corrected to 15% O_2, the differences between the operating frequency are greatly reduced. This is reassuring and agrees with with the observations in Fig. 6 that the system can reliably capture integral values, and the observed variations in the following sections are primarily due to sampling effects and not integration effects. As mentioned at the end of Sect. 2.2, oxygen correction amplifies the measurement scatter for 2 Hz due to the large O_2 content of the exhaust gas.

Figure 9 also shows NO concentrations measured parallel to NO_x, which indicates that the measured NO_x consists mostly of NO. Although the influence of the sampling method on the NO oxidation could not be quantified, this is in agreement to the findings of Yungster et al. (2006). There, only negligible amounts of NO_2were found *inside* the combustion tube, with the bulk of the observed NO_2 formed outside in the direct vicinity of the PDC exhaust after the ejected NO mixed with the surrounding air. Therefore, since NO_x and

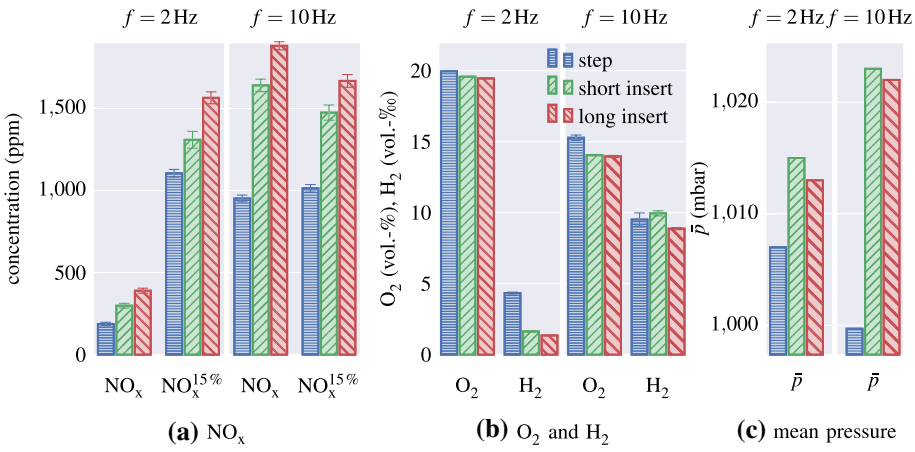

Fig. 10 Sample average of measured concentrations and sample mean pressure for varying outlet geometry

NO concentrations can be considered close to equivalent in the conditions found inside the PDC, the remaining analysis will focus on measurement values for NO_x.

3.3 Outlet Geometry

Ideally, the gas sample to be analyzed for pollutant levels should be taken at a position where fuel consumption is completed and that allows for consistent measurement of exhaust gas composition. However, due to the transient nature of the detonation cycle, gas dynamic effects such as reflected shock waves, rarefaction waves, and temporary back flow could influence the exhaust gas composition at the sampling probe location. This section therefore investigates three distinctive outlet configurations: step configuration, short insert and long insert, which have been introduced in Fig. 3.

Figure 10 shows the results of NO_x measurements for these configurations for PDC operating frequencies of 2 Hz and 10 Hz. Since an operating frequency of 20 Hz resulted in measured NO_x concentrations above the upper limit of the CLD (2500 ppm), these results are not shown. It becomes obvious that the interaction of probe positioning and outlet geometry can have a significant impact on the measured NO_x emissions. This is the case for both measured and oxygen-corrected results.

When measuring with the short insert installed instead of the step design, an increase in NO_x in Fig. 10a is accompanied by an increase in sample line mean pressure in Fig. 10c as well as by a noticeable decrease in oxygen and hydrogen in Fig. 10b (the latter only for $f = 2$ Hz). The increase in mean pressure is a result of the combination of higher static pressure and increased dynamic pressure on the leading edge of the probe due to the elimination of the sudden expansion.

The gas sample collection is primarily defined by the instantaneous pressure difference between sample pump and combustion chamber. An increase in mean sample line pressure would therefore indicate an increase in mean sample mass flow. However, since the pressure increase is caused by additional kinetic energy of the gas, it is more likely to increase the sample rate only during periods of high flow velocity. These periods primarily consist of the detonation and subsequent exhaust stage of the PDC cycle before purge, which are also the stages of highest NO_x concentration inside the tube. However, this should also

result in a corresponding decrease in measured O_2 and H_2 which would compensate for any additionally measured NO_x when oxygen corrected values are employed. Although a slight decrease in O_2 and H_2 is observable, it is insufficient to explain the increase in measured NO_x by the above mentioned phenomenon.

This implies that higher measured NO_x does not solely result from unsteady sampling but could also be a result of a change in the state of the combusted gases before entering the sampling probe due to the change in outlet geometry. The sudden change in cross section interferes with every shock and expansion wave propagating across. Combustion products flowing downstream due to the expansion occurring after the detonation has left the tube are subject to a sudden pressure decrease when crossing the step. This potentially leads to a change in volume bias of the integral sample volume, which was shown before to be dependent on the pressure in the vicinity of the sampling probe. Slightly increased oxygen content for the step design in Fig. 10b and lower pressures in Fig. 10c match this observation, but could also signify the sampling of back flowing ambient gases or separation regions, which would be in line with the marked increase in sampled hydrogen for the 2 Hz case with the step design.

When comparing the results for the short and long insert, differences in emissions are not as large as for the step design. It has been shown in several studies that back flow of surrounding gases can occur during filling of the PDC (Hoke et al. 2006) as well as during the exhaust stage (Caswell et al. 2013). Since the influence of these back flows is more pronounced in the direct vicinity of the tube's exhaust and reaches the sampling location earlier if it is placed nearby, employing the long insert configuration should reduce possible errors in gas composition measurements. However, a potentially more important effect derives from the additional overall length of the combustion tube for the long insert. As a result, expansion waves in the wake of the detonation require more time to reduce pressure and temperature inside the combustion chamber and further accelerate the combustion products towards the exhaust. Thus, the residence time of these products at elevated pressures and temperatures is increased, leading to increased NO_x concentrations. This effect has also been discussed in detail in Yungster et al. (2006), where a continuous, albeit nonlinear increase of NO was seen for increased tube length.

Concluding from these observations, the influence of the outlet geometry on the composition of the sampled exhaust gas should not be underestimated. A sudden change in the combustion chambers geometry was shown to have a significant impact on measured NO_x concentrations. However, due to multiple possible interactions with the flow field and the combustion products during the PDC cycle, this effect is hard to quantify and such geometries should therefore generally be avoided. For a constant tube diameter, the residence time of the combustion products at elevated pressures and temperatures is governed to a large extent by the time required for the expansion waves emerging from the open end to reach the combustion products. Thus by changing the distance between the gas sampling location and the combustion tube exit, an increase in measured NO_x concentrations for longer tubes is observed. However, in addition to this more replicable effect, interference of the exhaust in the form of back flow and ambient air dilution can not be fully ruled out, which is why the long insert was chosen as the reference for subsequent emission measurements. This had the additional benefit of reducing the vibrational strains to the analyzing equipment (in particular the paramagnetic sensor, as mentioned in Sect. 3.1) by leading the exhaust pressure waves away from the measurement equipment. Future researchers should therefore endeavor to position their sampling probes far from such sudden expansions while also avoiding comparisons between measurements with significantly different downstream tube lengths (or at a minimum account for the differences in the blowdown times).

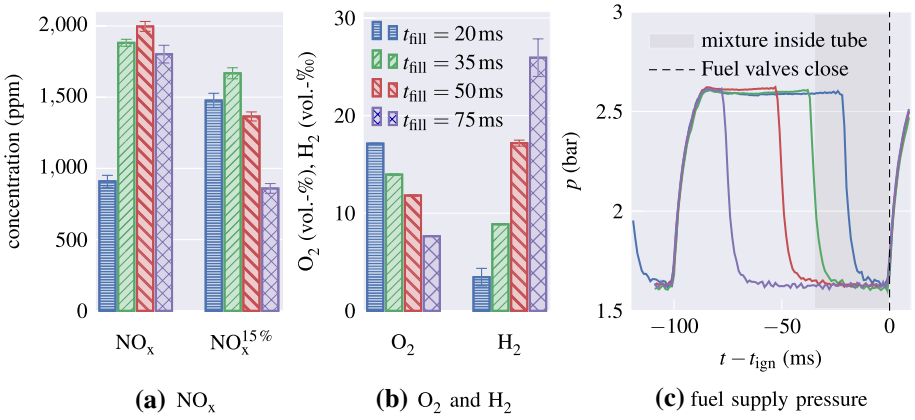

Fig. 11 Sample average of measured concentrations and pressure increase for varying t_{fill} at $f = 10\,\text{Hz}$

3.4 Fill Time

Some aspects of the impact of fuel charge length on NO_x emissions have already been discussed in Yungster et al. (2004, 2006), where charge length was varied by using combustion tubes of different lengths. For multi cycle operations with a fixed tube length, altering the fill time t_{fill} primarily changes the ratio of combustible gases to purge gases during one cycle. As already listed in Table 1, the current setup was operated with a constant air mass flow of 36.1 g/s, which requires an additional 1.055 g/s of hydrogen to be injected for stoichiometric combustion. This is equivalent to a mean flow velocity of 60 m/s. Since the overall test rig length including the DDT section and the long insert is 1.75 m, a fuel injection period of 35 ms has been used for the discussion so far, which results in a slight overfilling of the tube.

Figure 11 now investigates the resulting changes in measured gas composition if t_{fill} is altered for the long insert configuration at an operating frequency of 10 Hz. The apparent effect of reducing the fill time to 20 ms, and thus shortening the charge length, is to simultaneously reduce the ratio of combustion gases to purge air and to lower the combustion energy released with every cycle, because the detonation wave now only propagates through 2/3 of the overall tube before it decays to a pressure wave. This is in accordance with an increase in measured O_2 and decrease in measured H_2. Uncorrected NO_x concentration decreases, for the most part due to the air dilution, but some additional effects have to contribute as well.

The most prominent effect of increasing or decreasing t_{fill} is to alter the ratio of fill time to purge time. Increasing t_{fill} should result in an increase in measured H_2 and a decrease in measured O_2, which is confirmed in Fig. 11b. Since O_2 volume is thus effectively replaced by H_2 oxygen-corrected NO_x values decrease in Fig. 11a and no longer provide a meaningful comparison, because Eq. 6 is only valid for small traces of H_2 in the exhaust gas. While H_2 values in Fig. 11b appear to only exceed the upper limit of the analyzer of 2%vol for the longest fill time, short phases of sensor saturation that would distort the measurement result can be obscured by its cycle-averaged nature. This can be considered a general problem for any sort of post-process correction of emission measurements in cyclic combustion and it should therefore be ensured that no unknown gas quantities can distort measurements during operation.

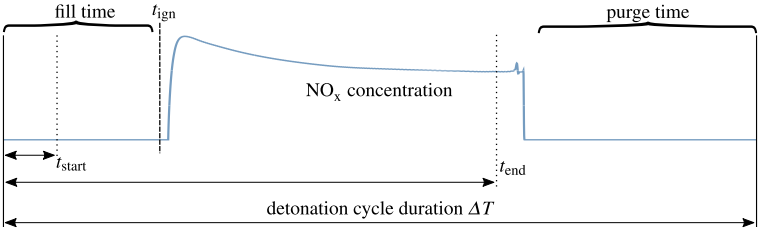

Fig. 12 Schematic temporal development of exhaust gases sampled by the probe for varied sample times

Overall, the additional volume of H_2 that is brought into each combustion cycle during the prolonged filling time causes NO_x concentrations to decrease. The slight increase in total NO_x from 35 to 50 ms in Fig. 11a could be caused by transient effects at the beginning of the fill time: Since the fuel injectors used in this study operate at a high upstream pressure, initial H_2 mass flow is larger as the pressure first needs to decrease before steady state conditions are reached after a few ms. This behavior is visible when investigating the fuel supply pressure upstream of the fuel injectors in Fig. 11c. After opening of the injectors, the sharply decreasing pressure requires a few milliseconds until a steady discharge pressure is reached. Since the momentary fuel mass flow into the combustion tube is directly linked to the supply pressure, this behavior leads to slightly richer mixtures at the tip of the package of combustible gas. As can be seen, increasing t_{fill} to 50 ms shifts this transient zone further away from ignition, causing the affected mixture to exit the combustion tube before the onset of detonation. The fuel remaining inside the tube would display an overall more homogeneous axial distribution, rendering the mixture more stoichiometric and thus resulting in increased total NO_x emissions.

3.5 Sampling Time Variations

Fig. 12 depicts a PDC cycle of duration ΔT as experienced by a sampling probe inside the tube to illustrate the possible impact of the chosen sample time window. Each cycle is composed of a filling phase t_{fill} containing the stoichiometric H_2–Air mixture, the combusted products that contain all the NO_x, and a subsequent purging state where the products are replaced by fresh air. The approximate time resolved NO_x curve depicted in Fig. 12 is derived from the same one-dimensional simulation of a detonation wave that has been used in Fig. 5b and illustrates the inhomogeneous axial distribution of NO_x within the combustion products. This distribution is not only caused by differences in NO_x concentration throughout the detonation cycle, but also by the fact that gas pressure and density are time dependent, with a maximum shortly behind the shock wave and a rapid decline once the exhaust stage sets in. It is easy to imagine that, by altering the sampling period $\Delta t = t_{end} - t_{start}$ and timing within this cycle, either by delaying the beginning of t_{start} or by ending it earlier at t_{end}, the outcome of the measurement of the NO_x concentration can be influenced. However, in what way this influence is reflected in the measured concentrations is unclear and is the scope of this section.

The sampling time variation is experimentally realized by employing a switching valve downstream of the sampling probe (see Fig. 4) that allows the probe to sample inert gas consisting of 25% CO_2 in Ar instead. This allows for maintaining a sufficient flow rate

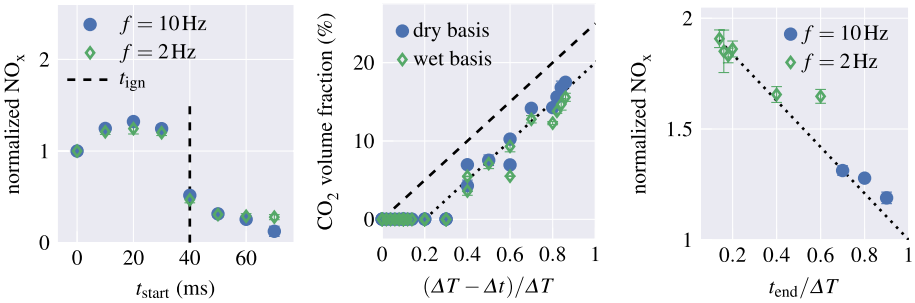

(a) Varying sampling start time **(b)** CO_2 content of sample **(c)** Varying sampling end time

Fig. 13 Influence of sample time variation on gas composition, NO_x emissions normalized by full sample result

within the analyzing section as well as to measure the concentration of dilution gas (by measurement of the resulting CO_2 concentration).

Figure 13 summarizes the findings from altering sampling start and end time, by comparing the resulting NO_x values for operating frequencies of 2 Hz and 10 Hz. Total measured NO_x concentrations are normalized by the result for a continuous sampling throughout the detonation cycle, i. e. $\Delta t = \Delta T$. The measured CO_2 volume fraction is used as an indicator for the amount of inert gas dilution. The latter was measured both for the dry and the wet line of the gas analyzer section, where values on a dry basis are necessarily higher due to the water vapor removal, thus also providing information about the sample's water content.

By looking at Fig. 13a it can be observed that delaying the sampling start while keeping $t_{end} = \Delta T$ causes an initial increase of measured NO_x by roughly 20%, followed by a steep decline for all cases where sampling only started after ignition had already occurred. The decline is plausible, because gas with high NO_x concentration and high pressure is effectively omitted from each cycle's gas sample.

The increase in NO_x for sample start times between 10 ms and 20 ms was initially unexpected. Essentially, delaying sampling from the combustion chamber during fill time replaces combustible mixture with the inert Ar–CO_2 mixture in the overall sampled gas volume for each cycle. Since both mixtures should not contain any NO_x, the observed increase can only be caused by a decrease of the total sample mass, rendering the relative amount of sampled NO_x larger. This implies that the omitted H_2–air mixture is not equivalently replaced by the inert gas. One explanation for this was found by analyzing the CO_2 content of the measured gas in Fig. 13b, where a noticeable increase of CO_2 in the gas sample is only seen for inert sampling times $> 0.2\Delta T$. This is most likely caused by the finite response time of the switching valve, leading to neither combustion gases nor inert gas being drawn into the analyzing section for the first 20 ms of each combustion cycle. An instantaneously reacting switching valve would result in measured CO_2 volume fractions following the dashed line, displaying a fully linear dependence from a sample containing 0% up to 100% of inert gas.

However, results for reduced sampling times by decreasing t_{end} that are displayed in Fig. 13c indicate that valve response time alone can not be responsible for the change in overall sample mass when switching to inert gas during the combustion cycle. Since ΔT is frequency dependent, the influence of t_{end} is shown only relative to ΔT for both frequencies.

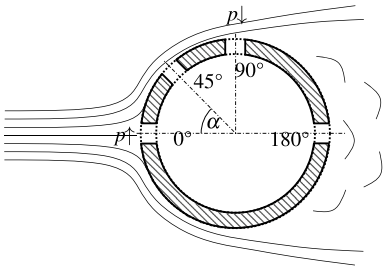

Fig. 14 Investigated angles for cylindrical probe in turbulent flow

A simple linear relation is found for $t_{end} > 0.2\Delta T$, with increasing NO_x concentrations for larger time periods of inert gas sampling. Even for measurements where combustion gases were drawn in only during the first 20% of each cycle, measured NO_x concentrations continued to rise when inert gas sampling was increased further. The results of Fig. 13a have already shown that NO_x formation is tied very strongly to the very short time frame of the propagating detonation wave and thus NO_x content of any ensuing gas flow can be neglected. So, as before, an increase in measured NO_x concentration when switching from one low-NO_x source to another can only be explained by a simultaneous decrease in overall sample mass. But as was shown in Fig. 13b, CO_2 content was already significant for these configurations, meaning that inert gas was clearly being collected by the analyzing system. This likely means that, even though it is collected by the sampling system, the mass of inert gas is unable to equivalently replace the gases that would otherwise be drawn from the combustion chamber during that time. This is a clear indication that (as was already argued in Sect. 2.2) the pressure increasing nature as well as the instationary flow field have a significant impact on the sampling process itself by influencing the momentary sampling mass flow.

Thus, constraining the sample time during the PDC cycle is only a viable option if the omitted gas volume is equivalently replaced by inert gas or the change in integral sample mass can be quantified in some way. Due to the strong influence of the instationary flow field of the PDC cycle on the sample mass flow, these requirements are hard to fulfill and a distortion of measured pollutant concentrations is therefore likely.

3.6 Sampling Probe Orientation

Switching between gas from the PDC cycle and inert purge gas in the last section has shown that the flow conditions in unsteady combustion systems like the PDC can influence the outcome of emission measurements. It can be expected that the fluctuating pressure field in the vicinity of the sampling probe in particular, resulting from static pressure changes as well as from the dynamic pressure of varying mass flows during each cycle, plays a major role in defining the momentary sample mass flow though the probe. The severity of this influence would thus also depend on the orientation of the sampling probe inlet relative to the bulk flow. Figure 14 depicts the inlet of a cylindrical probe that can be rotated in such a way that the angle between the inflowing gas velocity and the sampling orifice can be varied. Investigated angles were 0° (inlet at stagnation point, default configuration), 45°, 90° and 180°, as shown in Fig. 14.

In Fig. 15, temporal development of measured NO_x fractions over a PDC run time of 30 s is shown for operating frequencies of 2 Hz and 10 Hz and varied probe inlet angles. For

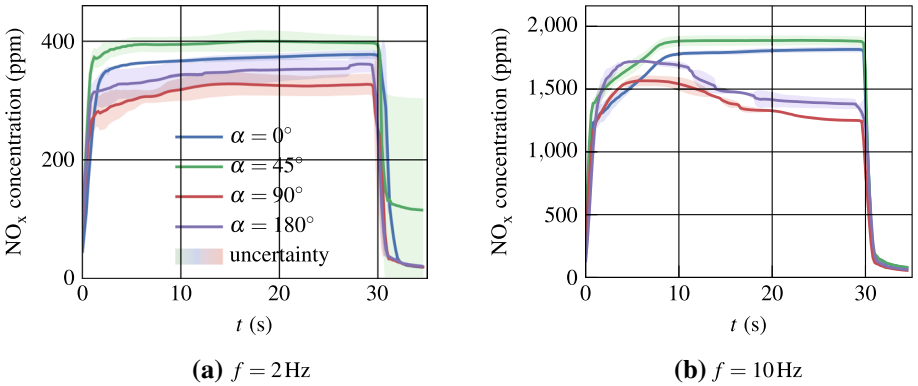

(a) $f = 2\,\mathrm{Hz}$ **(b)** $f = 10\,\mathrm{Hz}$

Fig. 15 Time development of measured NO_x concentration for varying PDC operating frequency and sample probe inlet's angle to flow direction

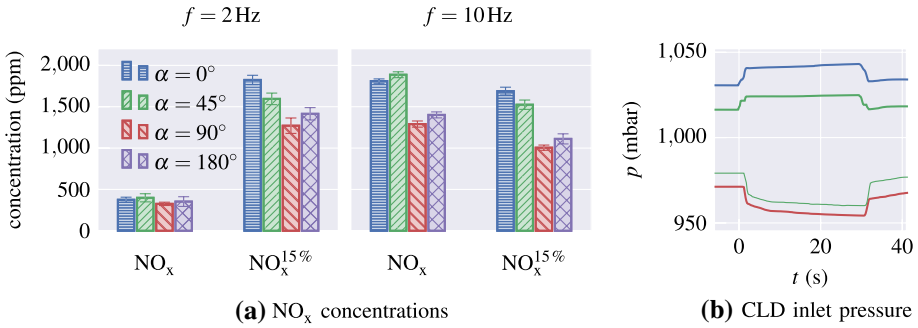

(a) NO_x concentrations **(b)** CLD inlet pressure

Fig. 16 Measured NO_x for varying probe inlet angle and CLD inlet pressure (for $f = 10\,\mathrm{Hz}$)

both frequencies, increasing the angle results in a small increase in measured NO_x for 45° and a decrease for larger angles. For 10 Hz, this decrease is very significant and is accompanied by a change in the temporal behavior, where NO_x values initially overshoot and then continuously decline towards a lower steady value.

Mean NO_x values from Fig. 15 together with the corresponding oxygen corrected data is shown in Fig. 16. Apart from the already discussed decrease in measured NO_x, it can be seen that differences for oxygen corrected NO_x between operating frequencies increases for larger angles.

Figure 16 sheds some light on the distinctly different behavior for larger flow angles at 10 Hz operating frequency: It depicts the absolute pressure measured at the inlet of the CLD analyzer before and during PDC operation. In accordance with the assumed flow field of Fig. 14, the initial pressure, which is purely induced by the total pressure resulting from the constant air flow before PDC operation begins, is highest for 0° where it is increased by the dynamic pressure of the flow. It is lowest for 90°, where no stagnation occurs in the vicinity of the sampling probe inlet. During the cycle stages of high gas velocity (detonation propagation and exhaust) the accelerated flow increases the pressure for the forward facing orientations, while decreasing that of the perpendicular and rear-ward facing orientations. This implies that the strong variations in pressure and velocity inherent to the detonation

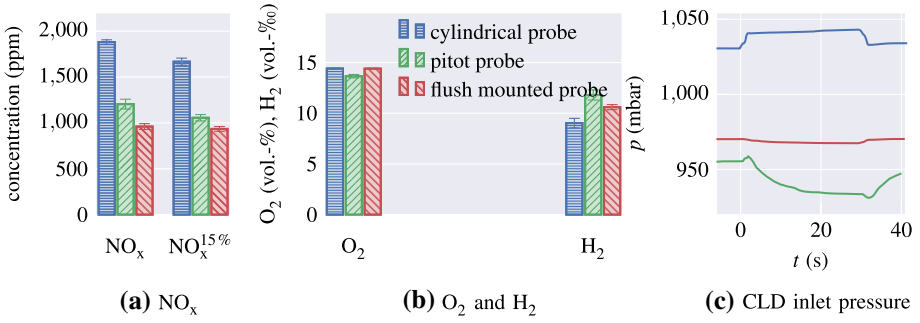

(a) NO_x **(b)** O_2 and H_2 **(c)** CLD inlet pressure

Fig. 17 Measured species concentrations for all three probe designs and CLD inlet pressure (for $f = 10$ Hz)

cycle increase the static pressure in the vicinity of the stagnation point on the leading edge of the probe and decrease the pressure along the leeward side of the separated flow. Since the sample mass flow is driven by pressure difference, altering this difference by changing the probe orientation aligned with transient pressure changes during every detonation cycle will alter the resulting proportion of gas sampling. It can be safely assumed in this case that the vacuum indicated in the sample line for angles > 45° only occurs during the times of highly accelerated gas flow after the passing of the detonation front and expansion of the combusted gases. Since this is also the period of highest NO_x concentration within the combusted gases, this attributes to the decrease in measured NO_x for these cases.

It is worth noticing that an inlet angle of 45° results in the highest uncorrected NO_x measurements for both operating frequencies, while correcting to 15% O_2 moves concentrations below those recorded for an inlet angle of 0°. This is caused by a significantly higher measured O_2 content for the case of 0°, which indicates the increased sampling of purge air compared to the 45° configuration.

3.7 Sampling Probe Design

The original cylindrical probe design, which had been chosen due to its robustness and ease of thermal control, had the downside of being rather intrusive with regards to the chamber flow field due to its high blockage ratio. Due to the large impact of the flow field on the sampling flow and by that on the measured concentrations that was found in the previous sections, it can be expected that the geometry and orientation of the probe in the measurement region can impact the measured concentrations. Thus, in addition, a pitot tube probe and a probe mounted flush with the combustion chamber wall were tested using the long insert outlet configuration and a PDC operating frequency of 10 Hz. The resulting NO_x concentrations are presented in Fig. 17, where they are compared to results obtained using the cylindrical probe. Additionally, O_2 and H_2 volume fractions and CLD inlet pressures are compared for all designs under the same operating conditions.

The measured NO_x emissions for the pitot and flush mounted probes are markedly lower compared to the cylindrical probe for uncorrected and oxygen corrected data in Fig. 17a, while oxygen content remains almost unchanged (Fig. 17b). When comparing the CLD inlet pressure in Fig. 17c, distinctive differences are observable: Due to its high blockage ratio, the cylindrical probe experiences a static pressure increase before operation of the PDC commences. Pressure increases again during PDC operation. The flush mounted

probe shows hardly any change in pressure during operation. Initial static pressure at the CLD inlet is slightly reduced for the pitot probe, which is caused by the increased flow resistance of its small, bend tip. During operation, flow resistance increases further due to the heating up of the tip, which further decreases sample line pressure. In contrast to the similar effect discussed in Sect. 3.6, here the pressure decrease occurs gradually over the course of the PDC run time. The primary reason for an increase in pressure for the cylindrical probe would be the significantly higher blockage ratio compared to the pitot tube.

Comparing these results with the ones from altering the probe inlet angle in Fig. 16a, it appears that the link found between sample line pressure and measured NO_x concentrations does not apply to the flush mounted probe, where pressure changes inside the combustion chamber are barely reflected in the sample line pressure and thus have limited influence on the sample mass flow and integral composition. Instead, measured NO_x concentration is very similar to the case of a cylindrical probe with an opening orifice perpendicular to the main flow, indicating that the reasons for the decreased concentrations are the same as discussed in Sect. 3.6.

Even though variations of pressure are to some extent undesirable for the emission sampling system, it has been shown in Sect. 2.2 that only a sampling mass flow that accounts for the variations inherent to the bulk mass flow is able to produce faithful integral emission values. This is a key difference between the cylindrical and pitot probe designs that collect their sample directly from the bulk flow center line in comparison with the flush mounted probe designs.

4 Summary

It was shown that even a highly unsteady system such as PDC allows for measurement of reasonably steady cycle-averaged emission values if given sufficient time. Dependence on operating frequency for a constant charge length is primarily related to the amount of dilution by purge gas between cycles and can thus be accounted for when correcting for a reference exhaust oxygen content (or similar means, such as considering the emission index), if dilution with O_2 is not too high. An equivalently effective measure would be the usage of emission index to indicate emission levels. However, both correction approaches can only account for dilution and are unable to account for the interaction of the sampling probe with the unsteady flow as was discussed above and will be summarized below.

A regular PDC cycle exhibits shock and pressure waves as well as expansion waves. This puts focus on the boundary condition of the detonation tube and possible interactions with a sampling probe if it is placed in the vicinity. To avoid unwanted effects from a change in combustor tube diameter, the sampling probe should be located sufficiently upstream of the combustor exit and far away from any changes in chamber geometry.

Varying fuel fill time and sampling periods can strongly influence emission measurements by altering the overall gas composition as well as the transient process controlling the collection of sample gases during one detonation cycle. Beside changing the composition, varying t_{fill} can also influence the axial distribution of equivalence ratio and the momentary flow field inside the detonation tube.

Small changes in sample timing can have a strong impact when these changes interfere with the occurrence of the detonation wave. As predicted in preliminary numerical studies in Hanraths et al. (2018), the bulk of NO_x is formed directly behind the front. Additionally, since the momentary sampling rate during each PDC cycle is strongly impacted by the

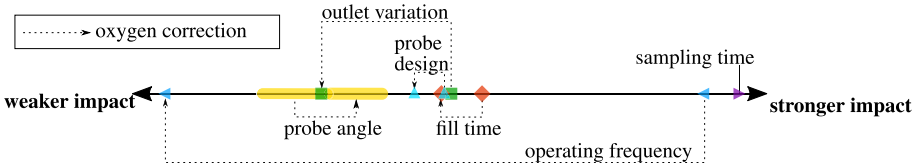

Fig. 18 Qualitative comparison of the the studied experimental parameters' impact on measured NO_x emissions, with and without oxygen correction

flow field inside the combustion chamber, switching to any idle purge gas supply for sampling during the cycle alters the overall sampling volume of which the integrated pollutant concentrations are derived. It thus distorts measurement results in a way that is difficult to quantify and should therefore be avoided.

The results for varying the sample probe inlet angle, as well as the design of the probe, have shown that changes of the flow field in the vicinity of the probe inlet influence sample gas composition. The reasons for this are most likely the combined effect of a change in the driving pressure difference between combustion chamber and analyzer as well as the deflection of the gas around the probe inlet. Naturally, an idealized gas sampling probe from a system with transient mass flow would be non-intrusive. At the same time, it should be able to account for the temporal changes in overall mass flow in the corresponding sample mass flow. This way it could be ensured that measurement would already be mass weighted and thus represent the actual amount of pollutants that was released to the environment. Practically, this would mean that a potentially less intrusive sampling positioning such as the flush mounted sampling probe might not be able to maintain a sufficiently proportional sample mass flow throughout the high velocity phases of the PDC cycle, as indicated by the decrease in measured NO_x concentrations. On the other hand, the sample line pressure of the flush mounted probe is less affected by pressure changes inside the combustion chamber, which would allow for a more stable sample mass flow, thus simplifying the interaction between combustion chamber and gas sample analyzer.

Figure 18 summarizes the results of this study by qualitatively showing the severity of the impact of the studied experimental parameters on the measured NO_x emissions. Also depicted by the dashed lines is how this impact is influenced by oxygen correction of the results.

It becomes clear that a variation of the sampling time should be avoided at all costs. While oxygen correction almost eliminates the frequency dependence of the measurements, its influence on the scale of other uncertainties is limited and it can even have adverse effects in the case of a variation of the probe inlet angle. That said, oxygen correction is overall beneficial and should be always used for emissions comparisons between PDC emissions measurements. Following oxygen correction and a steady, consistent sampling time, the most impactful parameters for researchers are a consistent filling time and probe design. Because these two parameters are likely to also show significant variability between laboratories, it is particularly important for researchers to carefully choose and report these parameters when presenting their results.

Even though this work focused on PDC, in principle, the results can be also applied to other technical applications that involve changes in flow field and chemical reactions on time scales that are irresolvable for subsequent gas analyzing systems. This includes single-cylinder test rigs of spark ignition engines used for the investigation of engine knock (a phenomenon that in itself can be closely tied to detonations in some cases) or per-cycle

variations in pollutant emissions from diesel and gasoline engines, which have gathered more interest lately due to more practical reference driving cycles in emission regulations (Karvountzis-Kontakiotis et al. 2017). Here, the definition of a sensible reference value that has to meet regulation values is a crucial topic as well. Pulse jets are another application closely related to PDC in terms of their operating frequencies and air-breathing operation. These conditions can introduce fast-changing flow conditions as well as air dilution that is difficult to quantify, especially when an ejector is applied (Williams et al. 2000). A similar concept, the shockless explosion combustion (SEC) relies on the auto-ignition of a spatially inhomogeneous fuel-air mixture triggered by acoustic pressure waves. Similar to PDC, each pulse jet or SEC operating cycle includes a purge phase to separate hot products from fresh gases, resulting in the same challenges when trying to adequately weight emission levels and maintain comparability with conventional combustion devices. The above discussions of the impact of probe design and positioning, sampling timing, and operating frequency are thus equally applicable and should be considered in the design of experiments and control measures.

5 Conclusion

Although crucial for eventual practical applications, the consideration of pollutant emission characteristics during the development of novel combustion concepts such as PDC is a topic which has not been as intensively discussed as other aspects. This is in part due to the fact that emissions measurements from instationary combustion in general, and pulse detonation combustion in particular, are a challenging task. The main reasons for this are short time scales, uncertainties in the exact state of the gases to be examined during sampling, the slow response of analyzing and sampling equipment, and techniques targeted towards continuous, steady state combustion systems. This study focused on understanding some of these challenges as well as potential sources of measurement error by considering a range of geometric and systematic parameters and their influence on NO_x emission measurements.

The goal of this work was to investigate and quantify possible impact factors on successful emission measurements from PDC. It was shown that care must be taken in ensuring experimental conditions that ensure a consistent flow interaction of the sampling probe with the unsteady mass flow within the combustion chamber. Practically, this means that small changes in overall geometry as well as the timing of the sample, which in contrast might be irrelevant in the case of stationary combustion, can influence measurement results in a way that is difficult to predict and should therefore be mitigated as much as possible. Fully quantitative comparability would therefore most likely require the development of a model burner with a more controllable, yet also less practical geometry. However, despite the cycle-averaged nature of any emission measurements in the context of PDC, operating conditions such as the frequency of ignition and the amount of purge gas can be accounted for by correcting the measured exhaust values accordingly.

Nevertheless, while absolute emission values retain a certain degree of uncertainty due to individual contributions of the effects summarized above, it has been shown that traditional gas sampling can be used to investigate the impact of changed operating conditions on NO_x emissions from unsteady combustion when the factors discussed above are considered.

Acknowledgements The authors gratefully acknowledge support by the Deutsche Forschungsgemeinschaft (DFG) as part of the research Grant 317741329.

Funding Open Access funding enabled and organized by Projekt DEAL.

Declaration

Conflicts of interest This study was funded by the German Research Foundation as part of the research Grant 317741329. The authors declare that they have no conflict of interest.

References

Anand, V., Gutmark, E.: A review of pollutants emissions in various pressure gain combustors. Int. J. Spray Combust. Dyn. **11**, 175682771987072 (2019). https://doi.org/10.1177/1756827719870724

Anand, V., Glaser, A., Gutmark, E.: Acoustic characterization of pulse detonation combustors. AIAA J. **56**(7), 2806–2815 (2018). https://doi.org/10.2514/1.J056204

Burke, M.P., Chaos, M., Ju, Y., Dryer, F.L., Klippenstein, S.J.: Comprehensive H2/O2 kinetic model for high-pressure combustion. Int. J. Chem. Kinet. **44**(7), 444–474 (2012). https://doi.org/10.1002/kin.20603

Caswell, A.W., Roy, S., An, X., Sanders, S.T., Schauer, F.R., Gord, J.R.: Measurements of multiple gas parameters in a pulsed-detonation combustor using time-division-multiplexed Fourier-domain mode-locked lasers. Appl. Opt. **52**(12), 2893 (2013). https://doi.org/10.1364/AO.52.002893

Council, E.: Directive 2010/75/EU industrial emissions. Off. J. Eur. Union **L334**, 17–119 (2010). https://doi.org/10.3000/17252555.L_2010.334.eng

Djordjevic, N., Hanraths, N., Gray, J., Berndt, P., Moeck, J.: Numerical study on the reduction of NOx emissions from pulse detonation combustion. Volume 4B: Combus. Fuels Emissions **140**(4), V04BT04A023 (2017). https://doi.org/10.1115/GT2017-64485

Döring, W.: Über den Detonationsvorgang in Gasen. Ann. Phys. **435**(6–7), 421–436 (1943). https://doi.org/10.1002/andp.19434350605

Driscoll, R., Randall, S., St. George, A., Anand, V., Gutmark, E.J.: Shock-initiated combustion in an air-breathing, pulse detonation engine-crossover system. AIAA J. **54**(3), 936–949 (2016). https://doi.org/10.2514/1.J054571

Frolov, S.M.: Natural-gas-fueled pulse-detonation combustor. J. Propuls. Power **30**(1), 41–46 (2014). https://doi.org/10.2514/1.B34920

Frolov, S.M.Y., Basevich, V., Aksenov, V.S., Gusev, P.A., Ivanov, V.S., Medvedev, S.N., Smetanyuk, V.A., Avdeev, K.A., Frolov, F.S.: Formation of nitrogen oxides in detonation waves. Russ. J. Phys. Chem. B **5**(4), 661–663 (2011). https://doi.org/10.1134/S1990793111040166

Giuliani, F., Lang, A., Irannezhad, M., Lundbladh, A.: Pulse detonation as an option for future innovative gas turbine combustion technologies: a concept assessment. In: 27th Congress of the International Council of the Aeronautical Sciences 2010, ICAS 2010, volume 4, pp. 2657–2666 (2010). ISBN 2006030876. https://doi.org/10.3354/meps08560

Gray, J.: Reduction in the Run-up Distance for the Deflagration-to-Detonation Transition and Applications to Pulse Detonation Combustion. PhD thesis, Technical University Berlin (2017)

Hanraths, N., Tolkmitt, F., Berndt, P., Djordjevic, N.: Numerical study on NOx reduction in pulse detonation combustion by using steam injection decoupled from detonation development. J. Eng. Gas Turb. Power **140**(12), 121008 (2018). https://doi.org/10.1115/1.4040867

Heiser, W.H., Pratt, D.T.: Thermodynamic cycle analysis of pulse detonation engines. J. Propuls. Power **18**(1), 68–76 (2002). https://doi.org/10.2514/2.5899

Hewson, J.C., Bollig, M.: Reduced mechanisms for NOx emissions from hydrocarbon diffusion flames. Symp. Combust. **26**(2), 2171–2179 (1996). https://doi.org/10.1016/S0082-0784(96)80043-9

Heywood, J.B.: Internal Combustion Engines Fundamentals. McGraw-Hill, Inc, (1988)

Hoke, J.L., Bradley, R.P., Gallia, J.R., Schauer, F.R.: The impact of detonation initiation techniques on thrust in a pulsed detonation engine. In: 44th AIAA Aerospace Sciences Meeting and Exhibit, pp. 1–12 (2006). https://doi.org/10.2514/6.2006-1023

Kailasanath, K.: Recent developments in the research on pulse detonation engines. AIAA J. **41**(2), 145–159 (2003). https://doi.org/10.2514/2.1933

Kailasanath, K.: Research on pulse detonation combustion systems: a status report. In: 47th AIAA Aerospace Sciences Meeting Including the New Horizons Forum and Aerospace Exposition, Number January, pp. 15–23, Reston, Virigina (2009). American Institute of Aeronautics and Astronautics. ISBN 978-1-60086-973-0. https://doi.org/10.2514/6.2009-631

Kailasanathk, K.: Review of propulsion applications of detonation waves. AIAA J. **38**(9), 1698–1708 (2000). https://doi.org/10.2514/2.1156

Karvountzis-Kontakiotis, A., Dimaratos, A., Ntziachristos, L., Samaras, Z.: Exploring the stochastic and deterministic aspects of cyclic emission variability on a high speed spark-ignition engine. Energy **118**, 68–76 (2017). https://doi.org/10.1016/j.energy.2016.12.026

Lisanti, Joel C., Roberts, William L.: Design of an Actively Valved and Acoustically Resonant Pulse Combustor for Pressure-gain Combustion Applications. In: 54th AIAA Aerospace Sciences Meeting, Reston, Virginia, jan 2016. American Institute of Aeronautics and Astronautics. ISBN 978-1-62410-393-3. https://doi.org/10.2514/6.2016-0899

Neumann, V., von Neumann, J.: Theory of detonation waves. In: Taub, A.J. (ed.) Collected works, vol. 6. Macmillan, New York (1942)

Paxson, D.E., Kaemming, T.: Influence of unsteadiness on the analysis of pressure gain combustion devices. J. Propul. Power **30**(2), 377–383 (2014). https://doi.org/10.2514/1.B34913

Qatomah, Mohammad, Lisanti, Joel C., Roberts, William: Influence of Fuel Composition on the Operation of a Liquid Fueled Resonant Pulse Combustor. In: 2018 Joint Propulsion Conference, Reston, Virginia. American Institute of Aeronautics and Astronautics (2018). ISBN 978-1-62410-570-8. https://doi.org/10.2514/6.2018-4571

Rasheed, A., Furman, A.H., Dean, A.J.: Experimental investigations of the performance of a multitube pulse detonation turbine system. J. Propul. Power **27**(3), 586–596 (2011). https://doi.org/10.2514/1.B34013

Rouser, K.P., King, P.I., Schauer, F.R., Sondergaard, R., Hoke, J.L., Goss, L.P.: Time-resolved flow properties in a turbine driven by pulsed detonations. J. Propul. Power (2014). https://doi.org/10.2514/1.B34966

Roy, G.D., Frolov, S.M., Borisov, A.A., Netzer, D.W.: Pulse detonation propulsion: challenges, current status, and future perspective. Prog. Energy Combust. Sci. **30**(6), 545–672 (2004). https://doi.org/10.1016/j.pecs.2004.05.001

Schauer, F., Bradley, R., Katta, V., Hoke, J.: Emissions in a pulsed detonation engine. In: 47th AIAA Aerosp. Sci. Meet. Incl. New Horizons Forum Aerosp. Expo., pp. 1–12, Reston, Virigina. American Institute of Aeronautics and Astronautics (2009). ISBN 978-1-60086-973-0. https://doi.org/10.2514/6.2009-505

U.S. Environment Protection Agency. Alternative Control Techniques Document - NOx Emissions from Stationary Gas Turbines (1993)

Völzke, F.E., Yücel, F.C., Gray, J.A.T., Hanraths, N., Paschereit, C.O., Moeck, J.P.: The influence of the initial temperature on DDT characteristics in a valveless PDC. In: Act. Flow Combust. Control 2018, pp. 185–196. Springer, Berlin, Heidelberg (2019). https://doi.org/10.1007/978-3-319-98177-2_12

Wang, K., Fan, W., Lu, W., Zhang, Q., Chen, F., Yan, C., Xia, Q.: Propulsive performance of a pulse detonation rocket engine without the purge process. Energy **79**(C), 228–234 (2015). https://doi.org/10.1016/j.energy.2014.11.017

Williams, T.C., Hargrave, G.K., Garner, C.P., Hanby, V.I.: Inlet mixing and nox formation in a helmholtz pulse combustor. Proc. Combust. Inst. **28**, 1 (2000). https://doi.org/10.1016/S0082-0784(00)80342-2

Xisto, C., Petit, O., Grönstedt, T., Lundbladh, A.: Assessment of CO2 and NOx emissions in intercooled pulsed detonation turbofan engines. J. Eng. Gas Turbines Power **141**(1), 011016 (2018). https://doi.org/10.1115/1.4040741

Yücel, F., Habicht, F., Bohon, M., Paschereit, C.: Autoignition in stratified mixtures for pressure gain combustion. Proc. Combust. Inst. **10**, (2020). https://doi.org/10.1016/j.proci.2020.07.108

Yungster, S., Breisacher, K.: Study of NOx formation in hydrocarbon-fueled pulse detonation engines. In: 41st AIAA/ASME/SAE/ASEE Jt. Propuls. Conf. & Exhib., Reston, Virigina (2005). American Institute of Aeronautics and Astronautics. ISBN 978-1-62410-063-5. https://doi.org/10.2514/6.2005-4210

Yungster, S., Radhakrishnan, K., Breisacher, K.: Computational and experimental study of NOx formation in hydrogen-fueled pulse detonation engines. In: 40th AIAA/ASME/SAE/ASEE Joint Propulsion Conference and Exhibit, pp. 1–17, Reston, Virigina (2004). American Institute of Aeronautics and Astronautics. ISBN 978-1-62410-037-6. https://doi.org/10.2514/6.2004-3307

Yungster, S., Radhakrishnan, K., Breisacher, K.: Computational study of NOx formation in hydrogen-fuelled pulse detonation engines. Combust. Theory Model. **10**(6), 23 (2006). https://doi.org/10.1080/13647830600876629

Zel'dovich, Y.: To the question of energy use of detonation combustion. J. Propul. Power **22**(3), 588–592 (2006). https://doi.org/10.2514/1.22705